Visual Abstract

Microstructural and mechanical characterization of a stainless-steel wire mesh–reinforced Al-matrix composite

P. Ferro, A. Fabrizi, F. Bonollo
University of Padova, Italy
paolo.ferro@unipd.it, https://orcid.org/0000-0001-8682-3486
alberto.fabrizi@unipd.it, https://orcid.org/0000-0002-7568-5804
franco.bonollo@unipd.it, https://orcid.org/0000-0002-7196-2886

F. Berto
Norwegian University of Science and Technology - NTNU, Norway
filippo.berto@ntnu.no, https://orcid.org/0000-0002-4207-0109

ABSTRACT. The microstructure and mechanical properties of stainless-steel AISI 304 wire mesh–reinforced AlSi9Cu-matrix composite specimens obtained by gravity casting were investigated. Optical and scanning electron microscope analyses were carried out on samples in both as-cast and solution heat treated conditions. The obtained results showed the absence of intermetallic phases at the insert/Al-matrix interface but even a significant fraction of lack-of-filling defects as well as lack-of-bonding areas that weekend the interface itself. The solution heat treatment, on the other hand, induced the precipitation of a thick and brittle intermetallic layer in the areas where a metallurgical bonding formed during casting. Moreover, the silicon particle spheroidization, improved the ductility of the matrix. The resulting microstructure allowed to obtain a slight improvement of elongation at failure of the compound casting compared to that of the aluminum alloy. Finally, basing on the obtained results, improvements are suggested that take into account both the preconditioning of the reinforcement surface and its geometry.

KEYWORDS. Al/Fe bimetallic castings; Interface; Intermetallic compounds; Microstructure; Mechanical properties.

OPEN ACCESS

Citation: Ferro, P., Fabrizi, A., Bonollo, F., Berto, F. Microstructural and mechanical characterization of a stainless steel wire mesh-reinforced Al-matrix composite, Frattura ed Integrità Strutturale, 55 (2021) 289-301.

Received: 29.11.2020
Accepted: 24.12.2020
Published: 01.01.2021

INTRODUCTION

Today we are living in the era of advanced materials. All materials families have reached high levels of performances. So that even polymers and ceramics are today used in structural applications. For the same reason, it is difficult for each single material to be able to undergo new significant improvements quickly. A breakthrough can be possible

only combining different materials to each other hence designing multi-material components. This is particularly urgent in view of the huge challenge linked to the climate change. With the aim at reducing gas emissions, reducing weights of mechanical components is mandatory. Thinking about the automotive and transport industry, lighter and lighter vehicles could be built by replacing steels with aluminum alloys [1]. These last in fact are characterized by a lower density, higher corrosion resistance and strength-to-weight ratio compared to steels. Unfortunately, with respect to steels, they have a lower stiffness and creep resistance so that they alone are not able to meet the requirements of the automotive industry. In this scenario, aluminum-steel bimetals could be a solution worthy of investigation. Different joining techniques are used to obtain such bimetallic components such as stir welding [2], friction welding [3], laser welding [4] and the most recent Hybrid Metal Extrusion & Bonding [5]. However, the most economical way to produce bimetallic components is pouring the liquid aluminum alloy into the mold cavity containing the steel reinforcement (compound casting). This allows also less geometrical restrictions compared to welding. Examples can be found in the production of engine cylinder blocks [6], crankcases or pistons [7,8] that uses particular techiques to reach a sound metallurgical bonding between the two metals such as vibration assisted casting [9], expandable pattern casting [10] or the 'Al-fin' process [11]. This is because in principle aluminum and iron are incompatible metals. Different thermal expansion coefficients, low mutual diffusivity and easy-to-form oxide or brittle intermetallic phases at the interface make difficult to obtain sound mechanical and metallurgical bonding. In particular oxide films on the steel insert and liquid aluminum surface [12,13,14] reduce the wettability of the steel surfaces to liquid aluminum while the brittle and thick intermetallic layers promote interfacial brittle fractures [15], thus compromising the metallurgical bonding. Despite these obstacles, the researchers were not discouraged and studied different strategies to obtain a good metallurgical bonding between the two metals. Jiang et al. used a 0.1 wt% Zn contained thin layer to protect the steel substrate from oxidation before pouring [16]. During pouring such thin layer completely dissolves into the liquid metal allowing a metallurgical bonding between the two materials and a significant increase of the shear stress of the bimetallic casting. The only issue is that Zn seems to promote an increase in the intermetallic compound growth reducing the insert/alloy interface strength [17]. In another work, the same authors [18] found that a double surface treatment consisting of immersion of the steel insert into an ammonium chloride solution at 80 °C followed by aluminizing (780 °C for 200 s) improved the shear strength of the two alloys interface of 40% compared to that of the untreated casting. The dominant intermetallic phase induced by aluminizing was found to be Al_5Fe_2 characterized by a tongue-like morphology [2]. A good metallurgical bonding was also obtained by nitride coating on the steel insert [19]. In this case, the nitride coating was also found to slow dawn the growth of the brittle intermetallic layer with positive effects on the interface mechanical strength. It is worth noting that iron reached intermetallic phases such as FeAl or Fe_3Al forms at higher temperatures compared to aluminum-reached ones like Al_5Fe_2, Al_2Fe Al_3Fe or Al_3Fe_3 and are even more desirable due to their better mechanical properties [20]. In this regard, with the aim at analyzing the mechanism of die soldering in aluminum die casting, Han and Viswanathan [21] measured a critical sticking temperature of 657 °C over which the intermetallic Al_3Fe forms at the contact surface between pure aluminum and mild steel. The presence of a high concentration of silicon in the aluminum alloy promotes the formation of a thinner layer of $Al_{4.5}FeSi$ that is detrimental because of its platelet morphology causing internal stresses in the insert/alloy interface [22, 23]. In particular, it was found that the growth rates of the intermetallic layer decreased when the Si content in the alloy was less than 1.5 wt%. On the opposite, the ternary Fe-Al-Si intermetallic phases appeared and grew quickly as the Si content in the molten metal increased to 2 wt% and 3 wt% [24,25]. The potential of Cu coating to inhibiting the intermetallic layer during stainless steel 308/aluminum alloy A319 compound casting production was explored by Khoonsari et al. [26]. They successfully found that Cu coating was effective against the intermetallic layer formation and worked better than the Zn protective layer.

Cast aluminum alloys undergo heat treatments such as solution followed by ageing to improve their mechanical properties. However, when dealing with aluminum-steel compound casting, such heat treatments could result very critical due to the metallurgical bonding alteration at the interface between the two coupled alloys. During solution treatment around 500 °C new intermetallic phases forms that according to their composition and thickness may increase or decrease the interface mechanical strength. Viala et al. [27] studied the possibility to produce bimetallic automotive components, made out of an Al–Si light alloy reinforced with a cast iron insert, by gravity die molding. Prior heat treatment, different kinds of intermetallic compounds were detected such as $\eta(Al_5Fe_2)$, $\tau_5(Al_{7.4}Fe_2Si)$ and $\tau_6(Al_{4.5}FeSi)$ and after solution heat treatment at 520 °C for 12h $\tau_2(Al_5Fe_2Si_2)$ and $\tau_{10}(Al_{12}Fe_5Si_3)$ also appeared. In particular, the excessive growth of the intermetallic compound η during solution treatment with the consequent formation of Kirkendall voids was attributed as the main cause of the insert/alloy interface bonding weakening. Similar results were reached even by Zhe et al. [28] after long-term (more than 40 hours!) solution treatments at 535 °C but in this case Kirkendall voids were observed to form in the intermetallic compound $\tau_6(Al_{4.5}FeSi)$. The thickness (x) of the reaction layer was found to increase during time (t) fallowing a parabolic growth law, $x^2 = Kt-b$, where b is a constant and K meets the Arrhenius type equation. The goal is to obtain a uniform intermetallic layer that doesn't exceed a few micrometers in order to guarantee a strong and tough bond [29]. Optimal heat treatment

process parameters were found by Jiang et al. [30] who improved the shear strength of the aluminum/steel bimetal by 39%, compared to that measured in the as-cast conditions, by a solution heat treatment at 500 °C for 2 hours. This was mainly attributed to the obtained morphology and size of the intermetallic compound $\tau_6(Al_{4.5}FeSi)$ that showed a not excessive growth and absence of crack defects. In a recent work [31], the influence of galvanization and heat treatment on the reaction layer between Al7SiMg and steel interface of a compound casting made out of low-pressure die casting was investigated. The authors found that a large amount of intermetallic phases form at the insert/alloy interface during casting with a prevalence of ternary $Al_{4.5}FeSi$ intermetallic particles (IMP). The reaction layer thickness increased significantly (80 μm) after heat treatment at 540 °C for 2h with cracks appearance that, *de facto*, weekend the interface bonding strength. The composition and microstructure of intermetallic compounds (IMC) formed at the interface between aluminum alloy AA4343 and stainless steel SUS316 upon annealing at 550 ◦C for 1h to 20h and at 610 ◦C for 15min to 10h were recently studied by Zhang et al. [32]. The reaction layer after solution at 550 °C for 10h was constituted above all by $\tau_{10}(Al_4Fe_{1.7}Si)$ and $\eta(Al_5Fe_2)$; its growth kinetics followed the rational equation $x = (kt)^n$, where x is the layer thickness, t is the time and k and n are two constants. Despite the great attention given by researchers to the steel/aluminum alloy interaction, only few works focused on the effective mechanical properties of such bimetallic materials. Haga et al. [33] characterized the mechanical properties of aluminum/steel wire-inserted composite strip reporting an improvement of the tensile strength of about 20%-30% compared to that of the aluminum matrix. By using a new short-flow process based on twin-roll casting (TRC) successfully developed to fabricate bimetallic laminated materials [34-36], Huang et al. [37] investigated the mechanical properties of stainless-steel wire mesh–reinforced Al-matrix composite plates. Due to the rapid solidification time that characterizes the process, the reaction layer was only 5 μm thick thus guarantying a good metallurgical bonding. Despite this, the mechanical strength was mainly influenced by the wire square mesh orientation with respect to the applied load direction since it has a great influence on the deformation compatibility. They found that both the tensile strength (with an improvement of about 30%) and elongation rate are best when the orientation angle was 45°.
The present study is useful to improve the mechanical properties in case of geometrical discontinuities [38-39] and can substantially impact on the final fatigue life at room [40-42] and high temperature [43] allowing to improve locally the strength to counterbalance local geometrical effects that can occur in a real 3D component [44-47].
Starting from the results of Huang et al. [37], the present work is aimed at studying metallurgical and static mechanical properties of a stainless-steel wire mesh–reinforced Al-matrix composite samples obtained by gravity casting that compared to TRC allows less geometrical restrictions. The effect of a solution heat treatment at 500 °C for 10 h was investigated, as well.

MATERIALS AND METHODS

Stainless steel wire mesh–reinforced Al-matrix composite samples were obtained by gravity casting. The insert was constituted by a stainless steel AISI 304 square mesh grid, where the wire diameter and pitch were 0.6 mm and 2.3 mm, respectively. The aluminum alloy was the AlSi9Cu (EN-AB 46400), which composition, measured with the optical emission spectrometer (Foundry Master Pro Oxford Instrument) prior and after pouring, is collected in Tab. 1.

AlSi9Cu	Al	Si	Cu	Zn	Fe	Mg	Mn	Ti	Cr	Pb	Ni
Before pouring	Bal.	9.25	1.05	0.624	0.502	0.439	0.292	0.135	0.0353	0.0291	0.0238
After pouring	Bal.	8.85	1.04	0.664	0.483	0.446	0.301	0.132	0.0364	0.0286	0.0218

Table 1: Chemical composition (wt%) of the aluminum alloy before and after pouring.

Fig. 1 shows the steel mold with the mesh and filter located inside before pouring. Following a similar procedure by Huang et al. [37], the wire mesh has been degreased using ultrasonic cleaning in acetone and then placed inside the mold cavity with an orientation angle (θ) of 0° relative to the load direction [37]. A thermocouple was also placed on mold surface in order to monitor and control the mold preheating temperature (350 ± 5°C). 12 samples were casted of which 6 without the steel insert. The alloy pouring temperature was 730 °C while the maximum mold temperature reached during all castings was 395.3 ± 3.4°C. The steel mesh positioning and eventual presence of macro defects in the obtained samples were first investigated by a non-destructive X-Ray radiography testing (RT). The metallurgical investigations were carried out on both transversal and longitudinal sections (Fig. 2) using the standard metallographic sample preparation. Optical (Leica LM2500) and scanning electron microscope (SEM, model Quanta FEG-250 of FEI©) were used for the microstructural characterization with particular attention to the bonding interface as well as the intersection between the longitudinal and latitudinal wires of the mesh. As shown in Fig. 2(a,b), two different transversal sections planes were prepared. Image

analyses aimed at measuring the volume of lack of filling closed to the wire mesh and the secondary dendrite arms spacing (SDAS) were carried out with the LAS software.

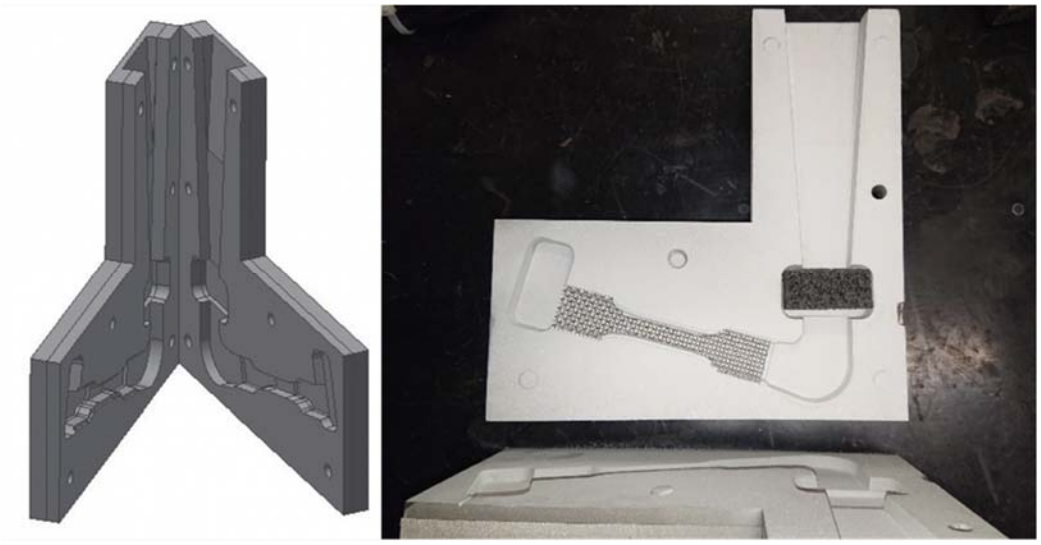

Figure 1: Mold geometry with insert and filter positioning

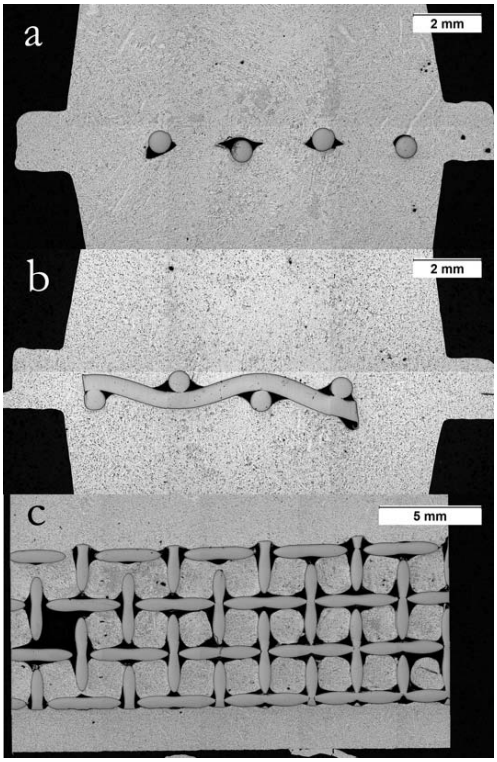

Figure 2: Transversal (a,b) and longitudinal (c) sections used for the metallurgical investigations.

The obtained castings underwent to machining to reach the target geometry for tensile tests schematized in Fig. 3. Tensile tests were performed using an MTS machine with an elongation rate equal to 4 mm/min. Finally, the effect of a solution heat treatment at 500 °C for 10 h on metallurgical and mechanical properties of the reinforced specimens were investigated.

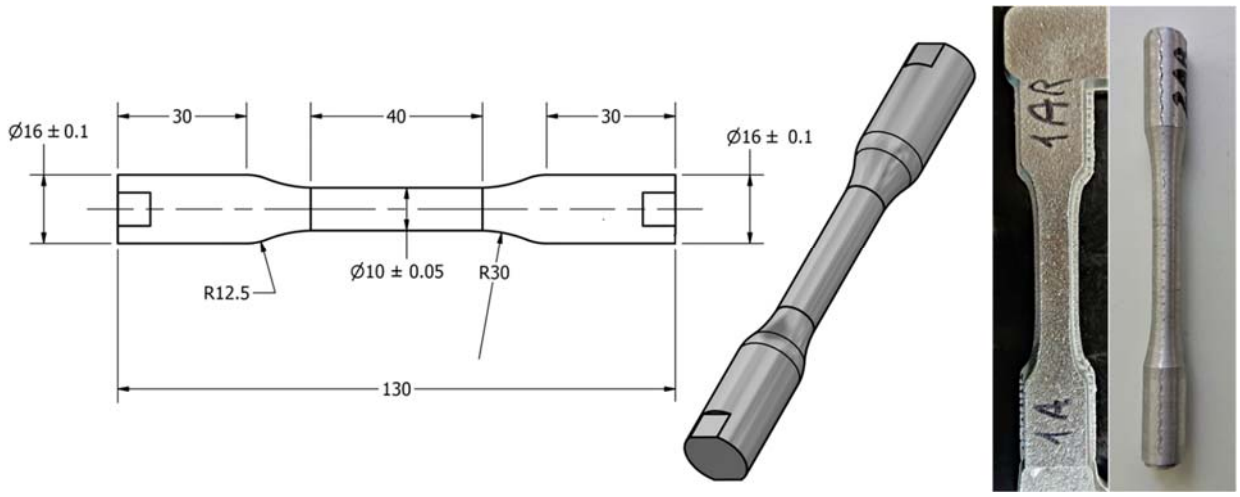

Figure 3: Geometry of tensile specimens (mm) and picture of a sample before and after machining.

RESULTS

Bi-material integrity and metallurgy

The RT was used to check the wire mesh has not be moved during pouring as well as the presence of macro-porosities. Fig. 4 shows an example of the obtained results. In most cases the wire meshes maintained their good centered position while residual voids were detected above all at wires intersections.

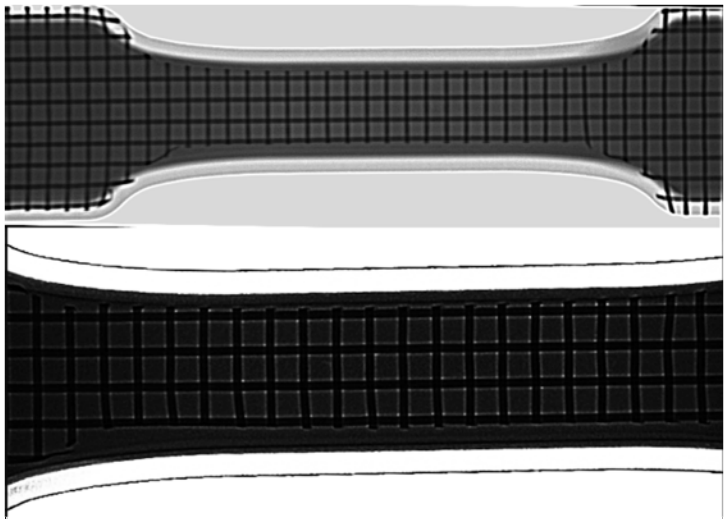

Figure 4: Results of radiography testing showing the wire mesh position and lack of filling at the wires intersection.

With the attempt to estimate the amount of residual voids, two zones were investigated close to the ends of the sample practical length. For each zone two transversal sections were observed, as shown in Fig. 2(a,b). It has to point out that large black zones as shown in the longitudinal section (Fig. 2(c)) were not taken into account since they are due to errors in sample preparations. The area fractions occupied by voids in the transversal and longitudinal sections were found to be 7.86% and (0.76±0.38)%, respectively. The lack of filling of matrix could be reduced or even avoided by improving the wettability between the molten aluminum alloy and steel wire or rising the casting temperature.

From 15 to 20 SDAS measurements were performed in order to obtain a good statistical value of such parameter. It was found a little decrease of the SDAS value of the aluminum matrix with the steel insert (22.10±1.89 μm) compared to that of the aluminum matrix without the reinforcement (25.71±1.85 μm).
Fig. 5 shows the microstructure of the aluminum matrix and reveals also some features of the interface Steel/Al. Some phases are well detectable such as Fe-rich precipitates (β-Al15FeS) and a quite low amount of Cu-rich phases. The optical micrograph in Fig. 5(a) reveals an interface with zones characterized by a metallurgical bonding and zones with a possible gap between the steel and the matrix. Fig. 5(b) shows at high magnifications the zone with a quite good contact between the two alloys where both the α-Al and the eutectic silicon are bonded to the stainless-steel wire.

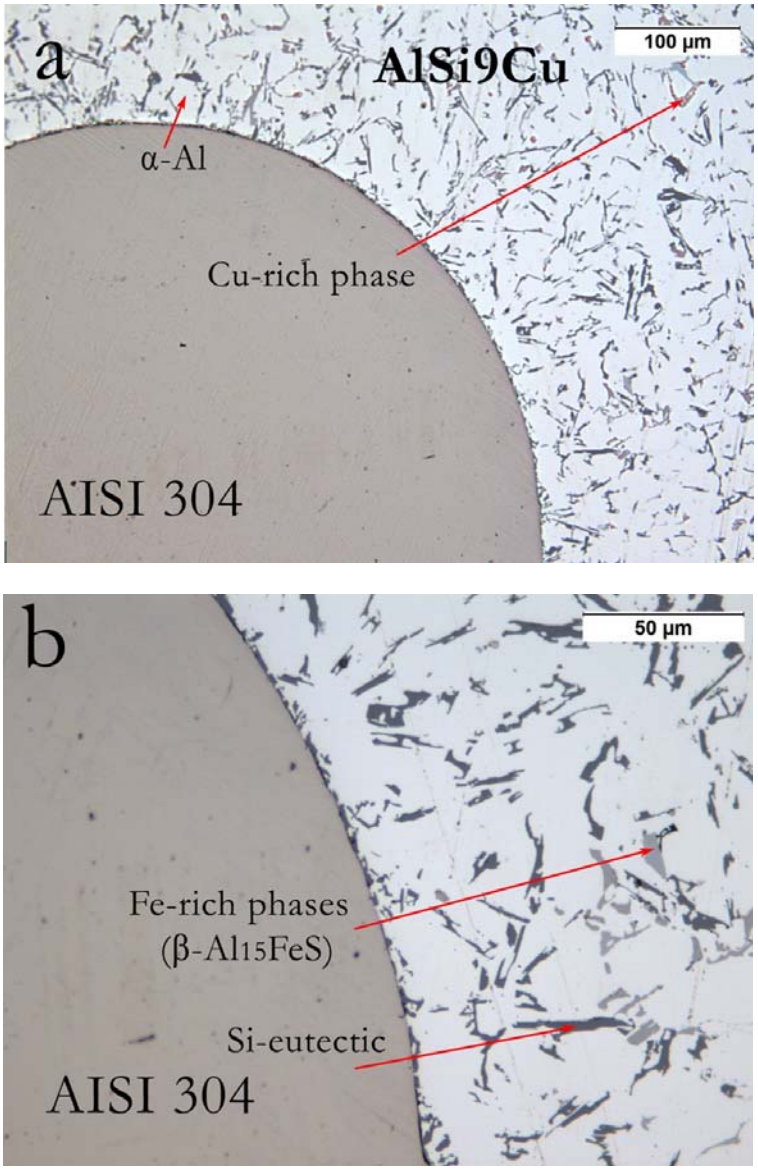

Figure 5: Optical micrographs of the two alloys and their coupling interface in the as-cast condition at different magnifications.

Using the scanning electron microscope, it was possible to better investigate the interface morphology of the as-cast sample (Fig. 6). In addition to the iron-rich precipitates visible in the aluminum matrix, using different magnifications it is possible to observe both lack-of-contact and good contact zones between the two alloys. After the solution heat treatment at 500 °C for 10 h, the insert/Al-matrix interface was partially decorated with an intermetallic substrate (Fig. 7). It is also observed how the eutectic silicon modified its morphology after the heat treatment from plate-like to almost equiaxed shape.

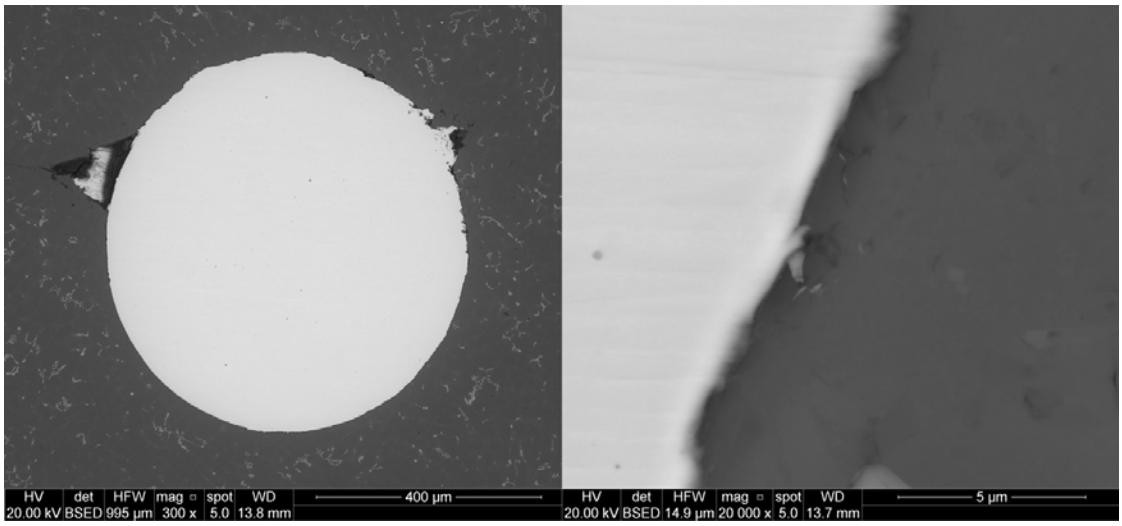

Figure 6: SEM micrographs of the two alloys and their coupling interface in the as-cast condition.

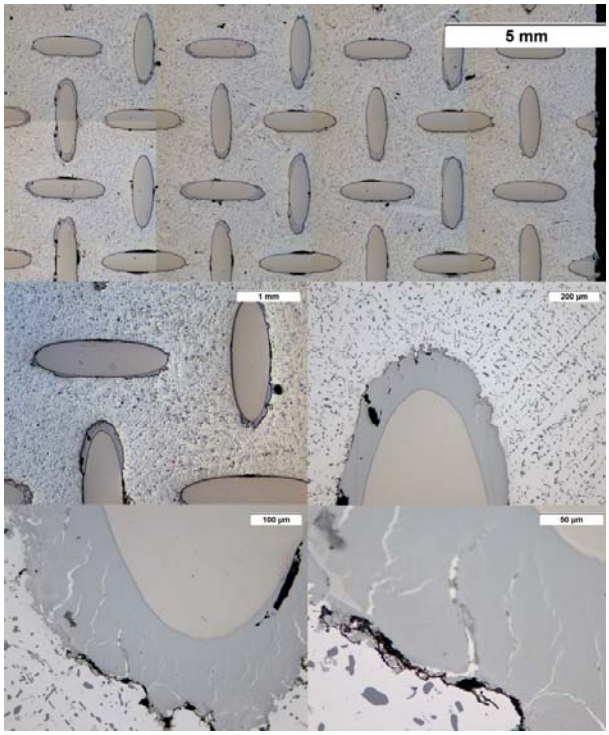

Figure 7: Optical micrographs of the two alloys and their coupling interface after solution treatment (500 °C, 10h).

Tensile tests

For the sake of simplicity, only one representative nominal stress-strain curve is shown in Fig. 8 for each condition. It is easy to observe that the steel wire mesh improved neither the mechanical strength (yield strength (YS) and ultimate tensile strength (UTS)) nor the elongation at fracture (A%) of the aluminum alloy in the as-cast condition. Only a little improvement of the Young's modulus (E) is obtained. On the contrary, the reinforcement slightly increases the UTS as well as the

elongation at fracture of the aluminum alloy in the solution heat treated condition. Moreover, the solution heat treatment decreases the mechanical strength but increases the ductility compared to those of the samples in the as-casting conditions. Tab. 2 summarizes the results of the tensile tests. It worth mentioning that all the tensile tests stopped as soon as the aluminum matrix broke.

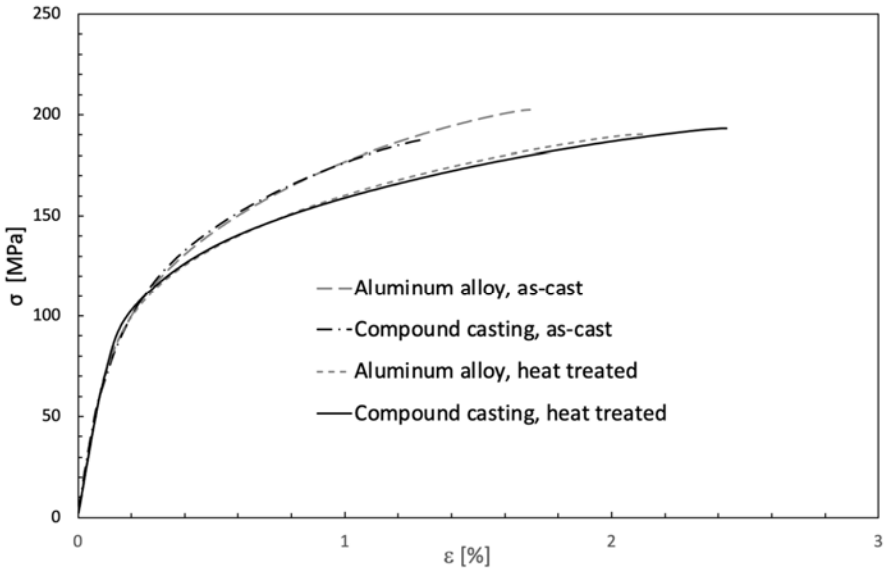

Figure 8: Stress-strain curves of the compound castings and Al alloy in different conditions.

	E [GPa]	YS [MPa]	UTS [MPa]	A [%]
Al matrix, as-cast	72.00±1.20	127.00±1.41	202.32±1.57	1.46±0.11
Al matrix + insert, as-cast	76.33±1.53	126.33±1.52	184.32±4.04	1.01±0.05
Al matrix, heat treated	74.50±0.71	122.50±0.76	191.00±1.41	1.89±0.03
Al matrix + insert, heat treated	74.67±1.48	122.67±1.03	194.68±1.52	2.34±0.05

Table 2: Comparison between the mechanical properties of the compound casting and the aluminum alloy.

DISCUSSION

Stainless steel wire mesh–reinforced Al-matrix composite specimens were obtained. The first issue is related to the significant percentage of residual voids at the V-shape narrow space at the intersection of steel wires and due to lack of filling. They in fact can easily trigger the crack propagation and above all the wire/matrix debonding. At the same time, they could be drastically reduced by increasing the casting temperature.

The steel wire mesh was found to influence the Al-matrix microstructure. As a matter of fact, it increased the grain refinement by increasing the cooling rate, as suggested by the SDAS measurements. Unfortunately, this grain refinement was not significant to obtain an increment of the mechanical strength in the as-cast condition, except for a slight increase in the yield stress that could be attribute to both the matrix refinement by grain refinement and the steel insert. The compound castings in the as-cast condition showed only a partial contact surface between the steel wire and the aluminum alloy (Fig. 5). Since the solidification and cooling times were short, no intermetallic phases were formed in those zones. On the other hand, according to the work of Huang et al. [37], Al-Fe interdiffusion is supposed to be occurred, promoting a metallurgical bonding. However, compared to Huang et al. [37] results, the metallurgical bonding didn't occur in all the wire surface probably because, using a gravity casting process instead of solid-liquid cast-roll bonding, the solidification front was more complicated resulting in complex shrinkages that could have generated same gaps between the wire and the aluminum alloy. Moreover, the presence of needle or plate shaped phases at the steel/Al interface (Fig. 5b) could further reduce the bonding strength [48]. The presence of lack-of-bonding areas in the as-cast condition is also confirmed by the intermetallic layer that formed during the solution heat treatment around the steel wires but obviously only at the prior

steel/aluminum contact zones (Fig. 7). The intermetallic layer does not cover the entire wire surface, in fact. Its high thickness (about 200 μm) is due to the long holding time at an elevate temperature during solution treatment, which allows new intermetallic layers to form through solid state diffusion. Kirkendall voids were also observed to form in the intermetallic compound as also reported by Zhe et al. [27] (Fig. 9). With reference to the work of Bakke et al. [30], the two intermetallic compounds were supposed to be β-$Al_{4.5}FeSi$ and/or τ_{10}-$Al_4Fe_{1.7}Si$. Finally, different cracks were observed in the intermetallic layer (Fig. 9) that confirm its brittle nature. They were attributed to the build-up of thermal stress at the interface during quenching due to the different thermal expansion coefficients of aluminum, steel and interfacial intermetallic phases, which results in cracks formation and propagation through the brittle intermetallic phases [49,50]. In such conditions, the steel/aluminum bonding is expected to be poor, as also reported in literature and confirmed by tensile tests.

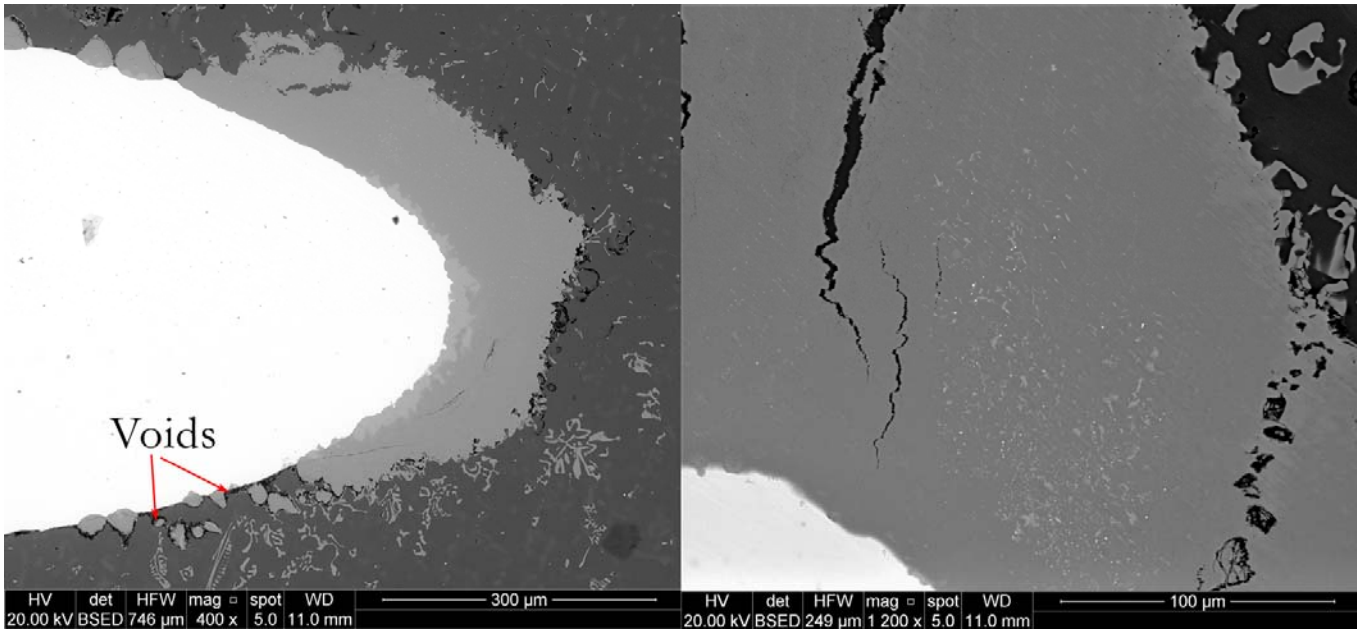

Figure 9: SEM micrographs of the intermetallic layer after solution treatment (500 °C, 10h).

Despite the different casting technology used, the present mechanical results are in good agreement with those found by Huang et al. [37]. As expected from metallurgical analyses, specimens fracture occurred only in the aluminum matrix (Fig. 10), proving an easy debonding and sliding of the steel wire mesh during the tensile test. However, the solution heat treatment, by increasing the ductility of the matrix through a silicon particles spheroidization, allows delaying the cracks initiation at the wire/Al interface therefore increasing the elongation at fracture of the Al/steel compound casting compared to that of the aluminum alloy (Tab. 2). It is interesting to observe the brittle fracture morphology of intermetallic layer. Fragments of the intermetallic layer are visible both in the steel and Al matrix surfaces (Fig. 10).

The results obtained in this investigation suggest different possible improvements. Process parameters, such as pouring and mold temperatures, should be optimized in order to eliminate voids due to lack of fusion. In this regard, also the kinetics of the solidification front could be investigated (say, through numerical simulation) and controlled in order to avoid debonding during the alloy solidification [51]. As a matter of fact, by controlling the solidification front is should be possible in principle to improve both the metallurgical and mechanical bonding [51]. The steel surface preconditioning is another design aspect to care about. According to literature [26], a Cu coating will result more effective, compared to Zn, against the intermetallic layer formation. Finally, another parameter worthy of investigation and improvement is the insert geometry. In fact, by optimizing the roughness and shape of the mesh, it will be possible to improve the Al/steel mechanical bonding, eliminate difficult-to-fill zones and above all, to design an insert stiffness closer to that of the alloy:

$$\left(\frac{E_{Insert}A_{Insert}}{L}\right)\simeq\left(\frac{E_{Matrix}A_{Matrix}}{L}\right) \quad (1)$$

In Eqn. (1) E is the Young's modulus, A is the cross section and L is the practical length.

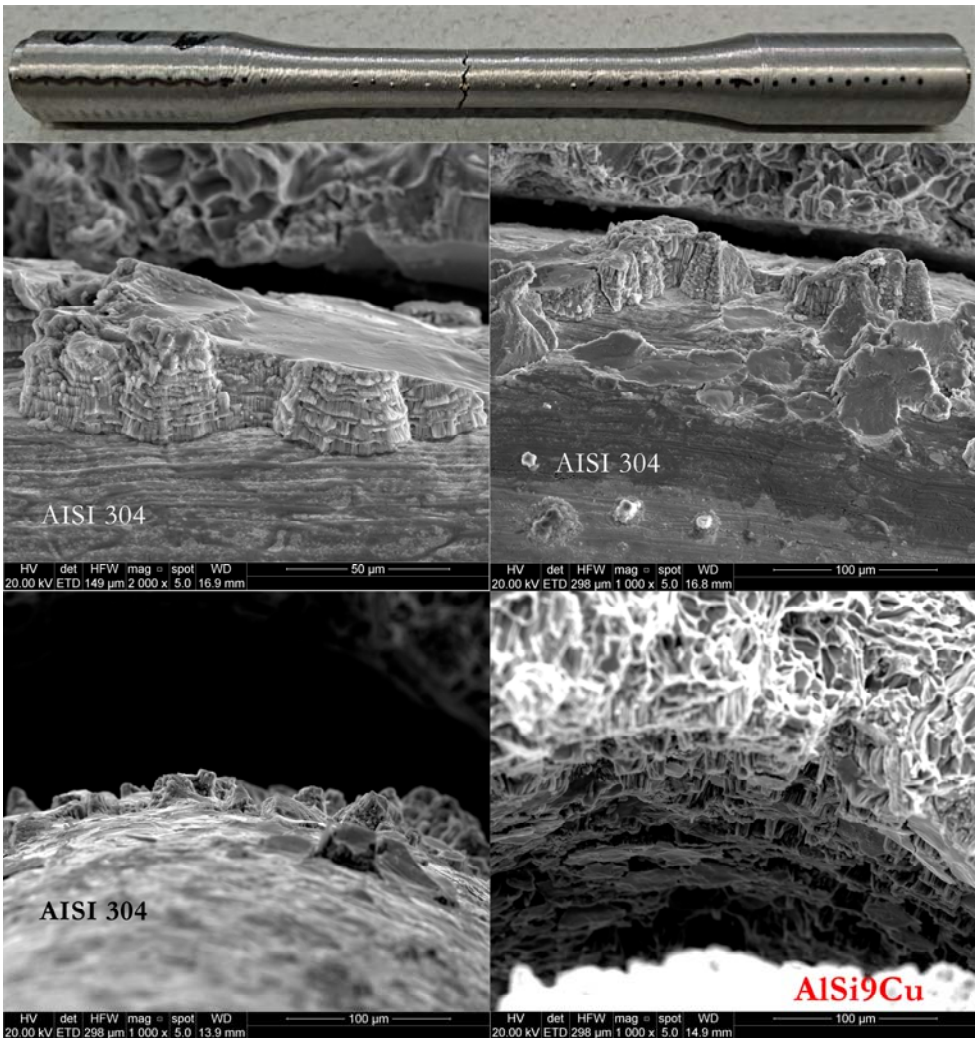

Figure 10: Broken sample in the as-cast condition and SEM micrographs of the Steel/Al interface after heat treated specimen failure.

This last effect (Eq. 1) was already highlighted by Huang et al. [37] who found improvements by simply rotating the steel wire mesh by 45° relative to the rolling direction. However, authors think that even better results could be obtained by further improving the insert design, taking advantage of additive manufacturing technologies and process simulation [], as well.

Conclusions

The microstructure and mechanical properties of stainless-steel wire mesh–reinforced Al-matrix composite specimens obtained by gravity casting were investigated. Moreover, the effect on metallurgical transformations and mechanical properties of a solution heat treatment at 500 °C for 10 hours were studied. Metallurgical investigations carried out on the as cast samples showed the absence of intermetallic phases at the insert/Al-matrix interface but even a significant fraction of lack-of-filling defects and lack-of-bonding areas. This compromised the interface strength that wasn't able to transfer the load from the matrix to the reinforcement. The solution heat treatment, on the other hand, induced the precipitation of a thick and brittle intermetallic layer in the areas where a metallurgical bonding formed during casting. Moreover, the silicon particle spheroidization, improved the ductility of the matrix. The resulting microstructure allowed to obtain a slight improvement of elongation at failure of the compound casting compared to that of the aluminum alloy.

Finally, basing on the results of the present work, possible improvements were suggested that take into account not only the insert surface preconditioning but also its geometry aimed at improving the alloy filling, the mechanical bonding and its stiffness that should be comparable with that of the matrix.

ACKNOWLEDGEMENTS

Authors would like to thank Mr. Giacomo Mazzacavallo for his precious support during metallurgical investigations as well as tensile tests.

REFERENCES

[1] Miller, W., Zhuang, L., Bottema, J., Wittebrood, A., De Smet, P., Haszler, A., Vieregge, A. (2000). Recent development in aluminum alloys for the automotive industry, Mater. Sci. Eng. A 280, pp. 37-49. DOI: 10.1016/S0921- 5093(99)00653-X.

[2] Springer, H., Kostka, A., dos Santos, J.F., Raabe, D. (2011). Influence of intermetallic phases and Kirkendall-porosity on the mechanical properties of joints be- tween steel and aluminium alloys, Mater. Sci. Eng. A 528, pp. 4630-4642. DOI: 10.1016/j.msea.2011.02.057.

[3] Herbst, S., Aengeneyndt, H., Maier, H.J., Nürnberger, F. (2017). Microstructure and mechanical properties of friction welded steel-aluminum hybrid components after T6 heat treatment, Mater. Sci. Eng. A 696, pp. 33-41. DOI: 10.1016/j.msea.2017.04.052.

[4] Jia, L., Shichun, J., Yan, S., Cong, N., Junke, C., Genzhe, H. (2015). Effects of zinc on the laser welding of an aluminum alloy and galvanized steel, J. Mater. Process. Technol. 224, pp. 49-59. DOI: 10.1016/j.jmatprotec.2015.04.017.

[5] Berto, F., Torgersen, J., Grong, Ø., Sandness, L. and Ferro, P. (2018). Characterization of Hybrid Metal Extrusion & Bonding (HYB) joints of AA6082-T6 Aluminium Alloy and S355 Steel. Proceedings of 22nd European Conference on Fracture, ECF22, Belgrade, Serbia, 26-31 August.

[6] Miyamoto, N. et al. (2007). Insert Casting Component, Cylinder Block, Method for Forming Coating on Insert Casting Component and Method for Manufacturing Cylinder Block, U.S. Patent WO2007007826, 18 Jan 2007.

[7] Nunney, M.J. (2006). Light and Heavy Vehicle Technology, 4th ed., Butterworth-Heinemann.

[8] Bennett, S. (2009). Modern Diesel Technology: Diesel Engines, 4th ed., Thomson Delmar Learning, Division of Thomson Learning.

[9] Pan, J., Yoshida, M., Sasaki, G., Fukunaga, H., Fujimura, H. and Matsuura, M. (2000). Ultrasonic Insert Casting of Aluminum Alloy, Scripta Mater., 43(2), pp. 155-159.

[10] Choe, K.H., Park, K.S., Kang, B.H., Kim, K.Y., Lee, K.W. and Kim, M.H. (2008). Study of the Interface Between Steel Insert and Aluminum Casting in EPC, J. Mater. Sci. Technol. (Shenyang, China), 24(1), pp. 60-64.

[11] Guertler, G. (1969). Compound Casting, Aluminium (Isernhagen, Germany), 45(6), pp. 368-373.

[12] Aylward, G., Findlay, T. (2002) SI Chemical Data, fifth ed., John Wiley & Sons Australia, Milton.

[13] Papis, K.J.M., Loeffler, J.F., Uggowitzer, P.J. (2009). Light metal compound casting, Sci. China, Ser. A 52, pp. 46-51.

[14] Papis, K.J.M., Hallstedt, B., Lo€ffler, J.F., Uggowitzer, P.J. (2008). Interface formation in aluminum-aluminum compound casting, Acta Mater. 56, pp. 3036-3043. DOI: 10.1016/j.actamat.2008.02.042.

[15] Springer, H., Kostka, A., Payton, E.J., Raabe, D., Kaysser-Pyzalla, A., Eggeler, G. (2011). On the formation and growth of intermetallic phases during interdiffusion between low-carbon steel and aluminum alloys, Acta Mater. 59, pp. 1586-1600. DOI: 10.1016/j.actamat.2010.11.023.

[16] Jiang, W., Fan, Z., Li, G., Li, C. (2016). Effects of zinc coating on interfacial microstructures and mechanical properties of aluminum / steel bimetallic composites, J. Alloys Compd. 678, pp. 249-257.

[17] Springer, H., Szczepaniak, A., Raabe, D. (2015). On the role of zinc on the formation and growth of intermetallic phases during interdiffusion between steel and aluminum alloys, Acta Mater. 96, pp. 203-211. DOI: 10.1016/j.actamat.2015.06.028

[18] Jiang, W., Fan, Z., Li, G., Li, C. (2015). Improved steel/aluminum bonding in bimetallic castings by a compound casting process. Journal of Materials Processing Technology, 226, pp. 25–31.

[19] Nazari, K.A., Shabestari, S.G. (2009). Effect of micro alloying elements on the interfacial reactions between molten aluminum alloy and tool steel, J. Alloys Compd. 478, pp. 523-530. DOI: 10.1016/j.jallcom.2008.11.127.

[20] Kobayashi, S., Yakou, T. (2002). Control of intermetallic compound layers at interface between steel and aluminum by diffusion-treatment, Mater. Sci. Eng. A 338, pp. 44-53. DOI: 10.1016/S0921-5093(02)00053-9.
[21] Han, Q., Viswanathan, S. (2003). Analysis of the mechanism of die soldering in aluminum die casting. Metallurgical and Materials Transactions A 34(1), pp. 139-146. DOI: 10.1007/s11661-003-0215-9.
[22] Cheng, W.-J., Wang, C.-J. (2011). Effect of silicon on the formation of intermetallic phases in aluminide coating on mild steel, Intermetallics 19, pp. 1455-1460. DOI: 10.1016/j.intermet.2011.05.013.
[23] Seifeddine, S., Johansson, S., Svensson, I.L. (2008). The influence of cooling rate and manganese content on the b-Al_5FeSi phase formation and mechanical properties of Al-Si-based alloys, Mater. Sci. Eng. A, 490, pp. 385-390. DOI: 10.1016/j.msea.2008.01.056.
[24] Yin, F.C, Zhao, M.X., Liu, Y.X., et al. (2013). Effect of Si on growth kinetics of intermetallic compounds during reaction between solid iron and molten aluminum, J. Transactions of Nonferrous Metals Society of China, 23, p. 556-561. DOI: 10.1016/S1003-6326(13)62499-1
[25] Wei, H., Fu-cheng, Y., Xu-ping, S. et al. Influence of silicon on growth kinetics of Fe_2Al_5 during reactive diffusion between solid iron and aluminum, J. Transactions of Materials and Heat Treatment, 31, pp. 28-32.
[26] Viala, J.C., Peronnet, M., Barbeau, F., Bosselet, F., Bouix, J. (2002). Interface chemistry in aluminium alloy castings reinforced with iron base inserts, Compos. Part A Appl. Sci. Manuf. 33, pp. 1417-1420. DOI: 10.1016/S1359835X(02)00158-6.
[27] Zhe, M., Dezellus, O., Gardiola, B., Braccini, M., Viala, J.C. (2011). Chemical changes at the interface between low carbon steel and an Al-Si alloy during solution heat treatment, J. Phase Equilibria Diffus. 32(6), pp. 486-497. DOI: 10.1007/s11669-011-9949-z.
[28] Durrant, G., Gallerneault, M. and Cantor, B. (1996). Squeeze Cast Aluminium Reinforced with Mild Steel Inserts, J. Mater. Sci., 31(3), pp. 589-602.
[29] Jiang, W., Li, G., Wu, Y., Liu, X., Fan, Z. (2018). Effect of heat treatment on bonding strength of aluminum/steel bimetal produced by compound casting, J. Mater. Process. Technol. 258, pp. 239-250. DOI: 10.1016/j.jmatprotec.2018.04.006.
[30] Bakke, A.O., Arnberg, L., Løland, J.-O., Jørgensen, S., Kvinge, J., Li, Y. (2020). Formation and evolution of the interfacial structure in al/steel compound castings during solidification and heat treatment. Journal of Alloys and Compounds 849, 156685. DOI: 10.1016/j.jallcom.2020.156685.
[31] Zang, X., Gao, K., Hu, X., Ding, Y., Wang, G., Wu, X., Nie, Z. (2020). Growth Kinetics of Interfacial Intermetallic Compound in Al(AA4343)/Steel(SUS316) Clad Strip. Materials Science Forum, 993, pp 447-456.
[32] Khoonsari, E.M., Jalilian, F., Paray, F., Emadi, F., Drew, R.A.L. (2010). Interaction of 308 stainless steel insert with A319 aluminium casting alloy. Materials Science and Technology, 26, pp. 833-841.
[33] Haga, T., Takahashi, K., Watari, H., et al. (2007). Casting of wire-inserted composite aluminum alloy strip using a twin roll caster. J. Mater. Process Tech., 192–193, pp. 108–113.
[34] Huang, H.G., Chen, P. and Ji, C. (2017). Solid-liquid cast-rolling bonding (SLCRB) and annealing of Ti/Al cladding strip. Mater. Design. 118, pp. 233–244.
[35] Bae, J.H., Rao, A.K.P., Kim, K.H., et al. (2011). Cladding of Mg alloy with Al by twin-roll casting. Scripta Mater. 64, pp. 836–839.
[36] Grydin, O., Gerstein, G., Nurnberger, F. et al. (2013). Twin-roll casting of aluminum–steel clad strips. J. Manuf. Process. 15, pp. 501–507.
[37] Huang, H., Wang, J., Liu, W. (2017). Mechanical properties and reinforced mechanism of the stainless steel wire mesh–reinforced Al-matrix composite plate fabricated by twin-roll casting. Advances in Mechanical Engineering, 9(6), pp. 1–9.
[38] Ayatollahi, M.R., Rashidi Moghaddam, M., Razavi, S.M.J., Berto, F. (2016). Geometry effects on fracture trajectory of PMMA samples under pure mode-I loading, Engineering Fracture Mechanics, 163, pp. 449–461. DOI: 10.1016/j.engfracmech.2016.05.014.
[39] Torabi, A.R., Campagnolo, A., Berto, F. (2015). Local strain energy density to predict mode II brittle fracture in Brazilian disk specimens weakened by V-notches with end holes Materials and Design, 69, pp. 22–29. DOI: 10.1016/j.matdes.2014.12.037.
[40] Zhu, S-P., Yu, Z-Y, Correia, J., De Jesus, A., Berto, F. (2018). Evaluation and comparison of critical plane criteria for multiaxial fatigue analysis of ductile and brittle materials, International Journal of Fatigue, 112, pp. 279-288. DOI: 10.1016/j.ijfatigue.2018.03.028.

[41] Correia, J., Apetre, N., Arcari, A., De Jesus, A., Muñiz-Calvente, M., Calçada, R., Berto, F., Fernández-Canteli, A. (2017). Generalized probabilistic model allowing for various fatigue damage variables, International Journal of Fatigue Volume 100, pp. 187-194. DOI: 10.1016/j.ijfatigue.2017.03.031.

[42] Ferro, P., Lazzarin, P., Berto, F. (2012). Fatigue properties of ductile cast iron containing chunky graphite, Materials Science and Engineering A, 554, pp. 122–128. DOI: 10.1016/j.msea.2012.06.024.

[43] Berto, F., Gallo, P., Lazzarin, P. (2014). High temperature fatigue tests of un-notched and notched specimens made of 40CrMoV13.9 steel. Materials and Design, 63(1), pp. 609–619. DOI: 10.1016/j.matdes.2014.06.048

[44] Berto, F., Lazzarin, P., Wang, C.H. (2004). Three-dimensional linear elastic distributions of stress and strain energy density ahead of V-shaped notches in plates of arbitrary thickness. Int. J. Fracture, 127(3), pp. 265–282. DOI: 10.1023/B:FRAC.0000036846.23180.4d

[45] Berto, F., Lazzarin, P., Kotousov, A. (2011). On higher order terms and out-of-plane singular mode. Mechanics of Materials, 43(6), pp. 332–341. DOI: 10.1016/j.mechmat.2011.03.004.

[46] Berto, F., Lazzarin, P. (2013). Multiparametric full-field representations of the in-plane stress fields ahead of cracked components under mixed mode loading, International Journal of Fatigue, 46, pp. 16–26. DOI: 10.1016/j.ijfatigue.2011.12.004.

[47] Wu, W., Hu, W., Qian, G., Liao, H., Xu, X., Berto, F. (2019). Mechanical design and multifunctional applications of chiral mechanical metamaterials: A review, Materials and Design, 180, 107950. Doi: 10.1016/j.matdes.2019.107950

[48] Seifeddine, S., Johansson, S., Svensson, I.L. (2008). The influence of cooling rate and manganese content on the b-Al5FeSi phase formation and mechanical prop- erties of Al-Si-based alloys, Mater. Sci. Eng. A 490, pp. 385-390. DOI: 10.1016/j.msea.2008.01.056.

[49] Jin, Y., Hong, S.I. (2014). Effect of heat treatment on tensile deformation character- istics and properties of Al3003/STS439 clad composite, Mater. Sci. Eng., A 596, pp. 1-8, https://doi.org/10.1016/j.msea.2013.12.019.

[50] Wang, Q., Leng, X.-s., Yang, T.-h., Yan, J.-c. (2014). Effects of FedAl intermetallic com- pounds on interfacial bonding of clad materials, Trans. Nonferrous Metals Soc. China 24, pp. 279-284. DOI: 10.1016/S1003-6326(14)63058-2.

[51] Soderhjelm, C., Appelian, D. (2018). Multi-Material Casting: Practical Foundry Guidelines. Modern Casting, June, pp. 40-43.

[52] Ferro, P., Berto, F. and Romanin, L. (2020). Understanding powder bed fusion additive manufacturing phenomena via numerical simulation. Frattura ed Integrità Strutturale, 14(53), pp. 252-284. DOI: 10.3221/IGF-ESIS.53.21.